Inorganic Chemistry

Article

pubs.acs.org/IC

Versatile Chemical Transformations of Benzoxazole Based Ligands on Complexation with 3d-Metal Ions

Olga Iasco,[†] Ghenadie Novitchi,[†,‡] Erwann Jeanneau,[†] Jean Bernard Tommasino,[†] Nans Roques,[§,⊥] and Dominique Luneau*[,†]

[†]Laboratoire des Multimatériaux et Interfaces (UMR 5615), Université Claude Bernard Lyon 1, 69622 Villeurbanne Cedex, France

[‡]Institute of Chemistry, Academy of Sciences of Moldova, Academiei, str. 3 MD-2028 Chisinau, Moldova

[§]LCC (Laboratoire de Chimie de Coordination), CNRS, 205 route de Narbonne, F-31077 Toulouse, France

[⊥]Université de Toulouse, UPS, INPT, LCC, F-31077 Toulouse, France

Supporting Information

ABSTRACT: Two benzoxazoles derivative ligands were synthesized from the condensation of 3,5-di-*tert*-butyl-*o*-benzoquinone (DTBBQ) with ethanolamine or 1,3-diamino-2-hydroxypropane in methanol. Condensation of DTBBQ with ethanolamine gives the expected 5,7-di-*tert*-butyl-2-methylenhydroxylbenzoxazole (**HL1**) while with 1,3-diamino-2-hydroxypropane it gives (2-hydroxyethyl-2-{2,4-bis(1,1-dimethylethyl)-1-phenol-6 amino}-2{5,7-di-*tert*-butyl-benzoxazole}) ($\mathbf{H_2L2}$) with only one benzoxazole ring instead of the symmetric *bis*-benzoxazole derivative. The structure of **HL1** and $\mathbf{H_2L2}$ were confirmed by NMR-spectroscopy and X-ray diffraction on a single crystal for **HL1**. The reaction of **HL1** with $CuCl_2$ gives a mononuclear $[\mathbf{Cu^{II}(HL1)_2Cl_2}]$ (**1**) complex for which the crystal structure shows that **HL1** is preserved. In contrast, upon reaction with nickel(II), cobalt(II), and manganese(II) $\mathbf{H_2L2}$ is further oxidized and transformed in new ligands **HL3** in mononuclear complexes $[\mathbf{M^{II}(L3)_2}]$ (M = Ni^{II} (**2**); M = Co^{II} (**3**)) and $\mathbf{H_2L4}$ in tetranuclear complex $[\mathbf{Mn^{II}_4(HL4)_4Cl_4}]$ (**4**) as found from the crystal structures of complexes **2**–**4**. Electrochemical studies for complexes **2** and **3** evidence complicated redox properties. $[\mathbf{Mn^{II}_4(HL4)_4Cl_4}]$ (**4**) has a cubane-like structure with a "4 + 2" fashion The magnetic susceptibility of **4** is well fitted considering one Mn---Mn interaction $J_a(Mn^{II}\text{-}Mn^{II}) = -0.50(1)$ cm^{-1} with $g = 2.00(7)$.

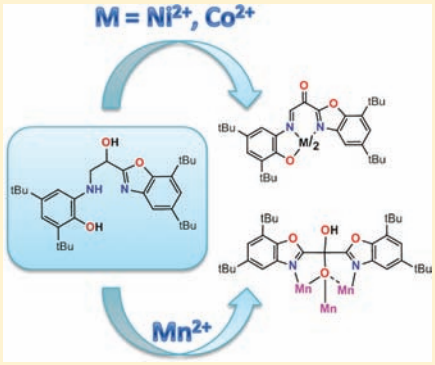

INTRODUCTION

The design of ligands and metal complexes with redox active properties has been an important field of investigation in coordination chemistry for many decades[1−10] and is still very active as shown by the recent dedicated forum in Inorganic Chemistry.[11−15] The development of molecular systems with such redox activity found direct interest as model in bioinorganic studies,[16−21] paramagnetic labeling,[22−25] or in catalytic applications.[26−30] An emblematic example is the work on semiquinone and catechol and derivatives.[3−5,8,9,14] Mononuclear[13,31,32] and dinuclear complexes of copper[33−35] as well as mononuclear[36] and dinuclear[16−19] iron with pro-radical catecholate and semiquinone ligands have been identified as intermediates in catalytic oxidations of catechols and phenol ligands. A main property associated with redox active ligands is the metal−ligand electron transfer. This may afford systems exhibiting valence tautomerism accompanied by reversible changes in magnetic and optical properties that are particularly attractive if one thinks of photoswitchable devices.[7−10,37]

In this context and also regarding our interest in single-molecule magnets (SMM), we investigated the coordination ability of benzoxazoles formed by condensation/oxidation reaction between 3,5-di-*tert*-butyl-*o*-benzoquinone (DTBBQ) and amines.[38−43] We have previously reported that the reaction of ethanolamine with DTBBQ gives 5,7-di-*tert*-butyl-2-methylenhydroxylbenzoxazole. This ligand was formed in situ in a one pot reaction with a mixture of Cu(II) and Ln(III) salts to give $[Ln_4Cu_8]$ systems.[42] When 1,3-diamino-2-hydroxypropane was reacted with DTBBQ instead of getting the corresponding symmetric bis-benzoxazole ligand we got an asymmetric ligand with only one benzoxazole moiety. Synthesis of the ligands, chemical transformations, and their 3d-metal complexes with structural, electrochemical, and magnetic properties studies are presented in this work.

EXPERIMENTAL SECTION

Materials. All chemicals and solvents were purchased from Aldrich and used without further purification. Manipulations were performed under aerobic conditions using chemicals and solvents as received.

Synthesis. HL1 (5,7-di-*tert*-butyl-2-methylenhydroxylbenzoxazole). Reaction between 3,5-di-*tert*-butyl-*o*-benzoquinone (DTBBQ) and ethanolamine was carried out under aerobic conditions at room temperature (Scheme 1). Ethanolamine (0.12 mL, 2 mmol) was added to a solution of DTBBQ (0.44 g, 2 mmol) in methanol (50 mL). The

Received: November 28, 2011
Published: January 10, 2012

   dx.doi.org/10.1021/ic202493z | *Inorg. Chem.* 2012, 51, 2588−2596

Scheme 1. Synthesis of HL1

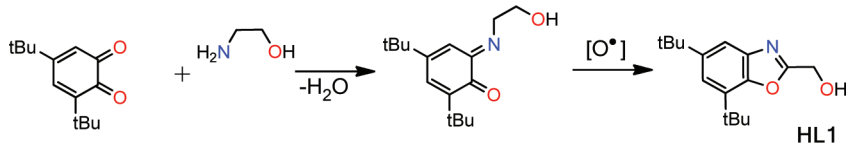

Table 1. Crystal Data and Structure Refinement Parameters for Compounds HL1 and 1−4

	HL1	$[Cu^{II}(HL1)_2Cl_2]$ (1)	$[Ni^{II}(L3)_2]$ (2)	$[Co^{II}(L3)_2]$ (3)	$[Mn^{II}_4(HL4)_4Cl_4]$ (4)
formula	C16H23NO2	$C_{32}H_{46}Cl_2CuN_2O_4$	$C_{62}H_{82}NiN_4O_6$	$C_{62}H_{82}CoN_4O_6$	$C_{124}H_{164}Cl_4Mn_4N_8O_{16}$
fw	261.35	657.18	1038.07	1038.25	2384.23
cryst. syst.	monoclinic	monoclinic	monoclinic	triclinic	monoclinic
space group	*P*2/*c*	*P*2/*n*	*P*2/*n*	*P*1	*C*2/*c*
a (A)	9.9461(8)	10.1542(6)	13.2714(9)	10.4757(9)	18.756(2)
b (A)	40.599(2)	11.812(8)	14.8637(6)	10.8700(10)	35.459(4)
c (A)	12.2510(10)	27.947(2)	17.3337(9)	27.854(2)	19.164(2)
α (deg)	90	90	90	83.040(6)	90
β (deg)	111.900(9)	96.970(5)	104.710(6)	80.938(6)	90.642(8)
γ (deg)	90	90	90	67.407(8)	90
V (Å^3)	4590.0(6)	3327(2)	3307.2(3)	2885.4(5)	12745(2)
Z	12	4	2	2	4
ρ_{calcd} (g/cm^3)	1.135	1.312	1.042	1.195	1.243
μ (mm^{-1})	0.584	0.854	0.339	0.350	0.533
T (K)	100(2)	100(2)	293(2)	110(2)	100(2)
R^a	0.0468	0.0517	0.0885	0.0913	0.0793
$R_w{}^b$	0.1351	0.1038	0.1352	0.2189	0.1651

$^aR_1 = \sum||F_o| - |F_c||/\sum|F_o|$. $^bR_{w2} = \{\Sigma[w(F_o^2 - F_c^2)^2]/[w(F_o^2)^2]\}^{1/2}$ and $[I > 2\sigma(I)]$.

resulting light green solution was stirred for 2−3 h. The final product **HL1** was isolated by chloroform extraction with followed chromatography on silica gel. Yield 29%. Anal. Calcd for $C_{16}H_{23}NO_2$: C, 73.53; H, 8.87; N, 5.36. Found: C, 74.06; H, 9.02; N, 5.25%. IR/cm^{-1}: ν_{max} 3199 (O−H), 2956, 2905, 2868 (C−H), 1578 (C═N), 1481 (C═C), 1403, 1361 (CH_3).

H_2L2 (2-hydroxyethyl-2-{2,4-bis(1,1-dimethylethyl)-1-phenol-6 amino}-2{5,7-di-*tert*-butyl-benzoxazole}). The reaction between DTBBQ and 1,3-diamino-2-hydroxypropane was carried out under aerobic conditions in refluxed methanol. To a solution of DTBBQ (0.44 g, 2 mmol) in methanol (50 mL) was added 1,3-diamino-2-hydroxypropane (0.09 g, 1 mmol). The resulting light green solution was stirred and refluxed for 2−3 h. After cooling **H_2L2** was isolated as a white precipitate which was filtered, washed with small amount of methanol, and dried under vacuum. Yield 39%; mp 200 °C. Anal. Calcd for $C_{31}H_{46}N_2O_3$: C, 75.26; H, 9.37; N, 5.66. Found: C, 74.84; H, 9.50; N, 5.71%. IR/cm^{-1}: ν_{max} 3369 (O−H), 2954, 2908, 2867 (C−H), 1589, 1573 (C═N), 1481 (C═C), 1403, 1357 (CH_3).

$[C^{II}(HL1)_2Cl_2]$ (1). The copper(II) complex **1** could be obtained starting from the ligand **HL1** or by a one pot reaction as it is described below. To a stirred solution of DTBBQ (0.44 g, 2 mmol) in acetonitrile (15 mL) at room temperature was added the equivalent quantity of ethanolamine (0.12 mL, 2 mmol). After 15 min of stirring, the solid $CuCl_2{\cdot}2H_2O$ (0.17 g, 1 mmol) was added to the reaction mixture. The resulting reddish solution turned dark green and was filtered. The filtrate was left undisturbed to concentrate slowly by evaporation. After one day green needle-like crystals of **1** were collected by filtration and washed with a small amount of MeCN. Yield: 42% (based on Cu). Anal. Calcd for $C_{32}H_{46}Cl_2CuN_2O_4$: C, 58.48; H, 7.06; N, 4.26. Found: C, 58.74; H, 7.07; N, 4.57%. IR/cm^{-1}: ν_{max} 3252 (O−H), 2958, 2869 (C−H), 1609, 1584 (C═N), 1440 (C═C), 1402, 1363 (CH_3).

$[Ni^{II}(L3)_2]$ (2). Solid $Ni(CH_3COO)_2{\cdot}6H_2O$ (0.125 g, 0.5 mmol) was added to a stirred solution of **H_2L2** (0.5 g, 1 mmol) in acetonitrile (20 mL) at room temperature. The resulting solution was stirred for 1 h then it was filtered and left undisturbed to concentrate slowly by evaporation. After 1−2 days, intense green-blue needle-like crystals of **2** were collected by filtration. Yield: 32% (based on Ni). Anal. Calcd for $C_{62}H_{82}N_4NiO_6$: C, 71.74; H, 7.96; N, 5.40. Found: C, 71.84; H, 7.87; N, 5.67%. IR/cm^{-1}: ν_{max} 2958, 2908, 2872 (C−H), 1678 (C═O); 1605 (C═N), 1494, 1445 (C═C), 1366, 1309 (CH_3).

$[Co^{II}(L3)_2]$ (3). The same procedure as for **2** was used with $Co(CH_3COO)_2{\cdot}6H_2O$ (0.125 g, 0.5 mmol) and **H_2L2** (0.5 g, 1 mmol). After 1−2 days green-blue intense needle-like crystals of **3** were collected by filtration. Yield: 36% (based on Co). Anal. Calcd for $C_{62}H_{82}N_4CoO_6$: C, 71.72; H, 7.96; N, 5.40. Found: C, 71.83; H, 8.02; N, 5.52%. IR/cm^{-1}: ν_{max} 3369 (O−H), 2958, 2904, 2869 (C−H), 1672 (C═O); 1623 (C═N), 1498, 1459, 1441 (C═C), 1359 (CH_3).

$[Mn^{II}_4(HL4)_4Cl_4]$ (4). Solid $MnCl_2{\cdot}4H_2O$ (0.2 g, 1 mmol) was added to a stirred solution of **H_2L2** (0.5 g, 1 mmol) in acetonitrile (20 mL) at room temperature. The resulting solution was stirred for 1 h; then it was filtered and left undisturbed to concentrate slowly by evaporation. After 5−7 days colorless needle-like crystals of **4** were collected by filtration. Yield: 25% (based on Mn). Anal. Calcd for $C_{124}H_{164}Cl_4Mn_4N_8O_{16}$: C, 62.47; H, 6.93; N, 4.70. Found: C, 62.32; H, 6.85; N, 4.89%. IR/cm^{-1}: ν_{max} 3191 (O−H), 2959, 2907, 2871 (C−H), 1607, 1572 (C═N), 1458 (C═C), 1404, 1365 (CH_3).

Physical Measurements. NMR spectra were recorded at 400 and 300 MHz on a Bruker DRX spectrometer in DMSO−D_6 solution. The chemical shifts were referred to TMS using the residual signals from the solvent.

IR spectra were recorded in the solid state on a NICOLET spectrophotometer in the 400−4000 cm^{-1} range.

Magnetic susceptibility data (2−300 K) were collected on powdered samples using a SQUID magnetometer (Quantum Design MPMS-XL), applying magnetic fields of 0.1 T. All data were corrected for the contribution of the sample holder and the diamagnetism of the samples estimated from Pascal's constants.[44,45] Magnetic data analyses were carried out including temperature independent paramagnetism, impurity contributions (ρ), and intermolecular interactions (zJ').

Minimization of magnetic susceptibility, derived from analytical calculation of energy levels associated with the spin Hamiltonians presented in the text, was carried out with Visualizeur-Optimiseur for

dx.doi.org/10.1021/ic202493z | Inorg. Chem. 2012, 51, 2588−2596

Matlab, using nonlinear least-squares of the Levenberg−Marquardt algorithm.[46,47]

Electrochemical measurements were performed using an AMEL 7050 all-in one potentiostat, using a standard three-electrode setup with a glassy carbon electrode, platinum wire auxiliary electrode and SCE (saturated calomel electrode) as the reference electrode. The complex solutions in CH_2Cl_2 were 1.0 mM, 2 mM, and 0.1 M in the supporting electrolyte n-Bu_4NPF_6. Under these experimental conditions, the ferrocene/ferricinium couple, used as an internal reference for potential measurements, was located at $E_{1/2}$ = 0.421 V.

X-ray Data Collection and Structure Refinement. Diffraction data were collected at 100.0(1) K using a Gemini A Ultra diffractometer from Agilent Technologies Ltd. (Mo Kα graphite-monochromated radiation, λ = 0.71073 Å) equipped with a CCD camera and controlled by the CrysAlisPro Software (Agilent Technologies, Version 1.171.34.49). A summary of the crystallographic data and structure refinement is given in Table 1. An analytical absorption correction was applied by modeling the crystal habit.[48] The crystals were placed in the cold stream of an Oxford Cryosystems open-flow nitrogen cryostat with a nominal stability of 0.1 K.[49] All the structures were solved by direct methods using the SIR97 program[50] and refined against F^2 using the CRYSTALS program.[51] All non-hydrogen atoms were refined anisotropically, whereas the hydrogen atoms were placed in ideal, calculated positions, with isotropic thermal parameters riding on their respective carbon atoms. The graphical manipulations were carried out with the DIAMOND[52] program. Selected bond distances and angles for **1**−**4** and **HL1** are listed in Table 2, Supporting Information, Table S1.

Table 2. Selected Bond Distances for 1−4

$[Cu^{II}(HL1)_2Cl_2]$ (1)		$[Ni^{II}(L3)_2]$ (2)	
Cl1−Cu1	2.284 (2)	N2−Ni1	2.071(4)
Cl2−Cu1	2.283 (2)	O3−Ni1	1.996(4)
O2−Cu1	2.502(2)	N1−Ni1	2.074(5)
O3−Cu1	2.523(2)		
N1−Cu1	2.069(2)		
N2−Cu1	2.021(3)		
$[Co^{II}(L3)_2]$ (3)		$[Mn^{II}_4(HL4)_4Cl_4]$ (4)	
O3−Co1	2.002(4)	N1−Mn1	2.213(5)
O4−Co1	1.996(4)	N2−Mn1	2.229(5)
O7−Co2	2.000(5)	N4−Mn2	2.284(5)
O12−Co2	2.017(4)	N3−Mn2	2.179(4)
N1−Co1	2.160(5)	Cl1−Mn1	2.39(2)
N2−Co1	2.136(5)	Cl2−Mn2	2.40(2)
N3−Co1	2.130(6)	Mn1−O3	2.198(4)
N4−Co1	2.138(5)	Mn1−O7	2.143(4)
N5−Co2	2.199(5)	Mn2−O3	2.169(4)
N6−Co2	2.137(5)	Mn2−O7	2.170(4)
N7−Co2	2.204(6)	Mn1---Mn2	3.361(4)
N8−Co2	2.133(5)	Mn1---Mn2′[a]	3.504(7)
		Mn1--- Mn1′[a]	3.731(3)
		Mn2---Mn2′[a]	3.705(8)

[a]Mn1′ and Mn2′ hold for position: (1 − x, y, 0.5 − z).

RESULTS AND DISCUSSION

HL1 (5,7-Di-*tert*-butyl-2-methylenhydroxylbenzoxazole) was synthesized in methanol by a condensation reaction between 3,5-di-*tert*-butyl-*o*-benzoquinone (DTBBQ) and ethanolamine in aerobic conditions[53] as it is well evidenced from ^{1}H and ^{13}C NMR spectroscopy (Supporting Information, Figure S3). In a first step the amino group of ethanolamine reacts with the less hindered carbonyl group from the first position of DTBBQ resulting in the formation of a Schiff-base (Scheme 1). Then the oxazole cyclization occurs because of successive oxidation (Scheme 1) as previously reported.[38,39]

Single crystals of **HL1** suitable for X-ray analysis were grown from chloroform solution. **HL1** crystallizes in the monoclinic $P2/c$ space group. The crystal structure consists of discrete molecules arranged in three symmetrically independent sites. One molecule of **HL1** is presented in Figure 1.

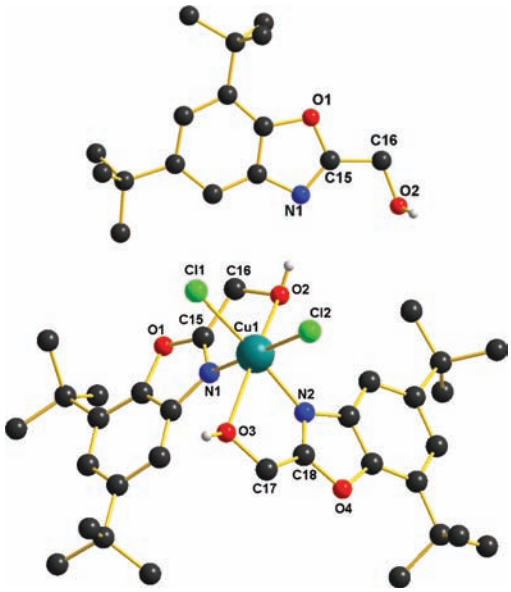

Figure 1. Crystal structure of **HL1** (top) and $[Cu^{II}(HL1)_2Cl_2]$ (**1**) (down). C−H hydrogen atoms are omitted for clarity.

Bond lengths and angles in the three **HL1** independent molecules are similar and consistent with distances and angles found in our previously reported heterometallic $[Ln_4Cu_8]$ clusters.[42] Distances for H_2C−OH bonds are in the 1.398−1.400 Å range, which is in agreement with a single bond between methylene carbon and hydroxyl group. The crystal packing of **HL1** is achieved through OH···N hydrogen bonds (2.755−2.794 Å) which give rise to a one-dimensional (1D) helical chain (Supporting Information, Figures S1, S2).

The reaction of DTBBQ with ethanolamine in presence of $CuCl_2{\cdot}2H_2O$ leads to the formation of the mononuclear copper(II) coordination compound $[Cu^{II}(HL1)_2Cl_2]$ (**1**). It could be also synthesized by reaction of **HL1** with $CuCl_2{\cdot}2H_2O$. **1** crystallizes in the monoclinic space group $P2/n$. The crystal structure consists of the mononuclear complexes (Figure 1). The copper(II) ion is coordinated by two nondeprotonated ligands **HL1** and two chloride ions. The metal center has a strong elongated *cis*-octahedral environment with a basal plane made of two nitrogen atoms from **HL1** (Cu−N bond lengths of 2.021; 2.069 Å) and two chloride ions (Cu−Cl bond lengths of 2.283; 2.284 Å). The apical positions are occupied by two oxygen atoms from **HL1** with Cu−O bond lengths of 2.502 and 2.523 Å. The axial distortions are typical for copper(II) complexes and caused by the Jahn−Teller effect.[54]

H_2L2 (2-hydroxyethyl-2-{2,4-*bis*(1,1-dimethylethyl)-1-phenol-6 amino}-2{5,7-di-*tert*-butyl-benzoxazole}) was obtained in methanol by reaction of DTBBQ with 1,3-diamino-2-hydroxypropane and has been characterized by NMR and IR-spectroscopy. Unexpectedly, this reaction does not result in the

dx.doi.org/10.1021/ic202493z | Inorg. Chem. 2012, 51, 2588−2596

Scheme 2. Chemical Transformation in the Synthesis of H_2L2

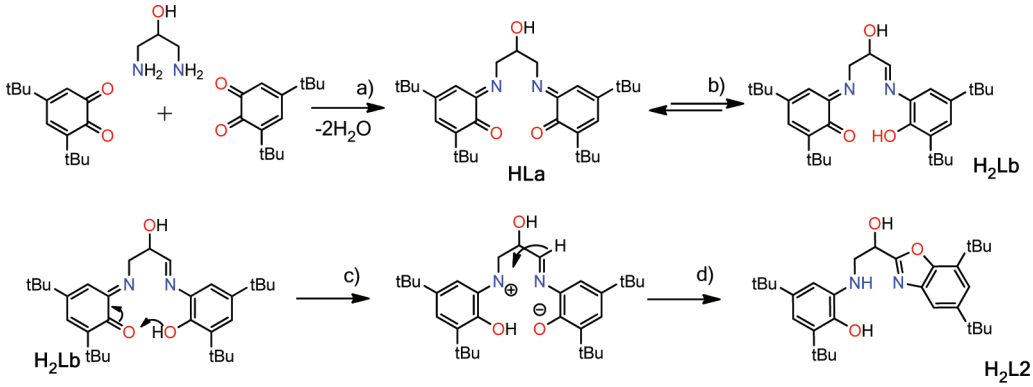

bis-benzoxazole analogue of **HL1**. The condensation of two amino groups of 1,3-diamino-2-hydroxypropane with carbonyl groups of two molecules of DTBBQ occurs as expected, but the following oxidation process results in the formation of only one benzoxazole cycle (Scheme 2). On the basis of previously reported works[38−41] the possible mechanism for the formation of **H_2L2** is presented in Scheme 2.

^{1}H NMR spectra (400 MHz) of **H_2L2** in d_6-DMSO shows 13 lines with well-defined hyperfine splitting. The NMR spectrum contains additional lines and is not consistent with the *bis*-Schiff base **HLa** (Scheme 2) or symmetrical *bis*-benzoxazole compound. The two-dimensional (2D) NMR spectroscopy was used to clarify the structure of **H_2L2**. According to ^{1}H NMR spectra the peaks in region of 1.1−1.5 ppm correspond to four methyl groups (with integral ratio of 3:3:3:3) (Supporting Information, Figure S4a). In ^{1}H−^{1}H COSY spectra these four signals do not have any cross picks. The spectral position of these signals and the absence of any superfine splitting allow assignment of these signals to *tert*-butyl groups from two magnetically non equivalent positions of two different aromatic rings, in agreement with condensation of two DTBBQ. The ^{1}H NMR spectra in the aromatic region (Supporting Information, Figure S4b) indicates the presence of two different di-*tert*-butyl substituted aromatic rings in **H_2L2**. According to the structure of **HL1** and other literature examples[38,39,41,55,56] the oxazole cyclization can be expected; however, the presence of two di-*tert*-butyl aromatic rings suggests that only one moiety of expected Schiff base was cyclized. A similar case with unsymmetrical benzoxazole cyclization has been reported for the reaction of 2-hydroxybenzaldehyde and 4,6-diaminoresorcinol in methanol.[43] On the other hand it has been reported that the condensation of DTBBQ with ethylenediamine or 2,2-dimethylpropylenediamine under aerobic conditions in acetonitrile only gives the symmetrical Schiff bases or their reduced amino form but no benzoxazole cyclization occurs in these conditions.

Thereby in 3.0−6.5 ppm region of ^{1}H−^{1}H COSY spectra five signals with chemical shift δ_H(ppm) 6.226(d); 5.005(dd), 4.836(t); 3.671(m), 3.476(m) and equal integral ratios are presented. The presence of the cross picks correlated with these five signals allows to assign them to protons of **HO**−C, O−**CH**; **NH**-C and two magnetically not equivalent N−**CH_2** protons as it is presented in Figure 2. The proposed assignments are consistent with ^{1}H−^{13}C HSQC (Figure 3) and ^{1}H−^{13}C HMBC (Supporting Information, Figure S5) NMR experiments and confirm the structure of **H_2L2**.

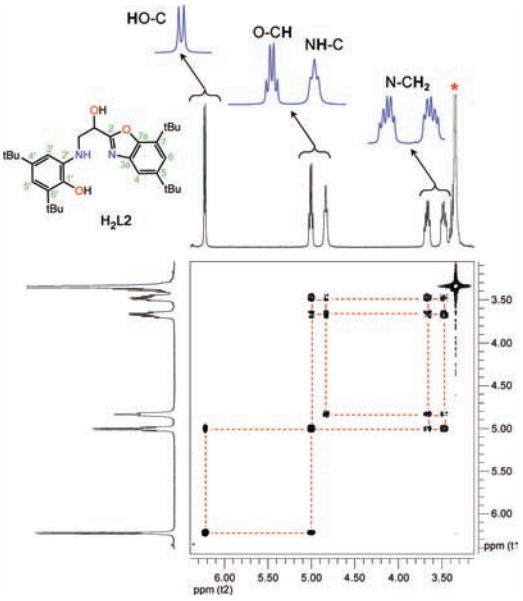

Figure 2. ^{1}H,^{1}H COSY NMR spectra (400 MHz) of **H_2L2** in D_6-DMSO solution. Blue lines correspond to expanded regions. Signal at 3.35 ppm corresponds to residual solvent H_2O. (see Supporting Information, Figure S4 for aromatic and *tert*-butyl regions).

The formation of **H_2L2** can be explained as a multistep process that involves a sequence of consecutive chemical transformations (Scheme 2). A similar mechanism was previously proposed for the interaction of DTBBQ with primary amines.[38,39] As for **HL1** the first step is the formation of symmetrical Schiff base because of the reaction of two amino groups of 1,3-diamino-2-hydroxypropane with the less hindered carbonyl groups of DTBBQ (Scheme 2a). In the following step, the solvated Schiff base undergoes a keto−enol tautomerism[57−59] (Scheme 2b). Then the deprotonation and intramolecular reorganization occur (Scheme 2c). Finally the benzoxazole cyclization leads to the formation of **H_2L2** (Scheme 2d).

Two aromatic rings in **H_2L2** are connected by a flexible -NH−CH_2−CH(OH)- chain which can have different conformations because of the free rotation around -H_aH_bC-(sp^3)---(sp^3)CH_c(OH). The analysis of the hyperfine splitting constants $^3J_{HaHc}$ and $^3J_{HbHc}$ correlated to the theoretical simulation of NMR spectra indicates that the most probable conformation in **H_2L2** corresponds to values of dihedral angles of 28.37° and 151.81° for H_cCCH_b and H_cCCH_a respectively

dx.doi.org/10.1021/ic202493z | *Inorg. Chem.* 2012, 51, 2588−2596

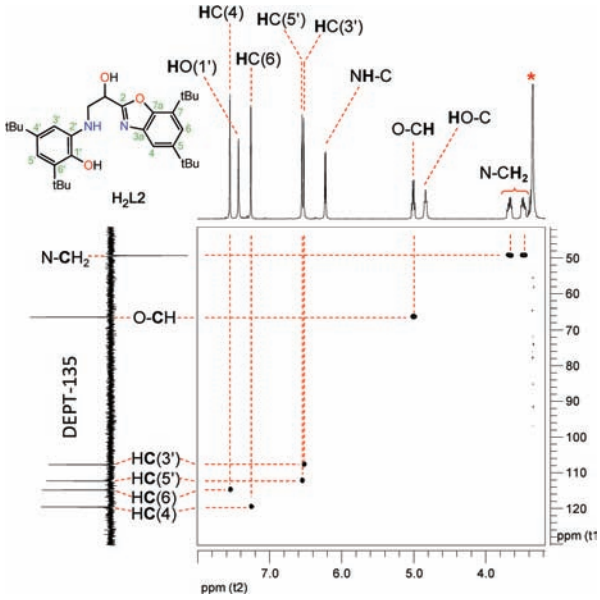

Figure 3. $^{1}H,^{13}C$ HSQC NMR spectra of $\mathbf{H_2L2}$ in D_6-DMSO solution. Signal at 3.35 ppm corresponds to residual solvent H_2O.

(Supporting Information, Figure S6). With this conformation the relative positions of the OH and NH are appropriated for the coordination of $\mathbf{H_2L2}$ to the metal centers as a tridentate chelating ligand. Following the coordination ability of this new asymmetric bensoxazole ligand ($\mathbf{H_2L2}$) was studied using different metal ions.

$[\mathbf{M^{II}(L3)_2}]$ (M = Ni (**2**), Co(**3**)) were obtained in acetonitrile as green-blue intense needle-like crystals by the reaction of $\mathbf{H_2L2}$ with nickel(II) or cobalt(II) acetate in a 2:1 ratio. Complexes **2** and **3** (Figure 4, Supporting Information,

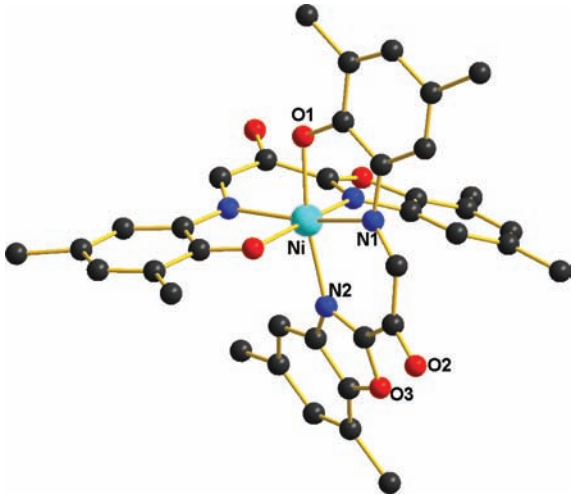

Figure 4. Molecular structure of **2**. Methyl groups and hydrogen atoms are omitted for clarity.

Figure S7) crystallize in monoclinic $P2_1/n$ and triclinic $P1$ space groups respectively. Because of the similarity of the molecular structure for the complexes **2** and **3** we will describe hereafter only the nickel analogue. The structure of **2** consists of the neutral mononuclear complex of nickel(II). The central atom is located on the 2 axis and coordinates with two ligands by two nitrogen atoms (N1, N2) and one oxygen atom (O3) resulting in a *cis*-octahedral (O_2N_4) environment (Figure 5). The central atom in **3** has the same coordination mode (Supporting

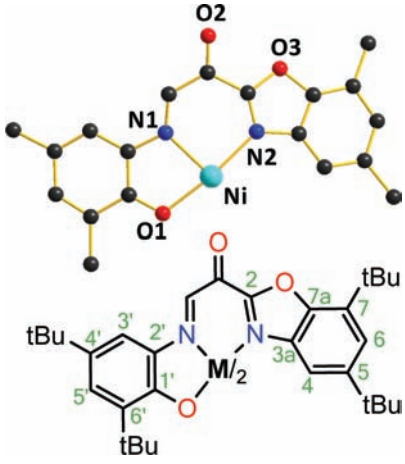

Figure 5. Coordination mode of **HL3** in **2**.

Information, Figure S7). The bond lengths analysis in the structure of **2** and **3** evidence the chemical transformation of the initial ligand $\mathbf{H_2L2}$ into a new **HL3** one during the reaction with cobalt(II) and nickel(II) (Scheme 3). In compound **2**, the bond lengths of 1.29 and 1.21 Å found for N1−C15 and C16−O2 respectively in compound **2** both correspond to double bonds in contrast with the single bonds observed in the initial $\mathbf{H_2L2}$. The distances of 1.221−1.325 Å were found for the same bonds in the Co(II) analogue (**3**). The oxidation of $\mathbf{H_2L2}$ upon the reaction with cobalt(II) and nickel(II) is also confirmed by appearance of the C═O band ($\nu_{(C=O)}$= 1675 cm^{-1}) and disappearance of the O−H large band in 3500−3000 cm^{-1} region in the IR spectra of **2** and **3** (Supporting Information, Figure S8). The catalytic oxidation of $\mathbf{H_2L2}$ into a **HL3** in presence of cobalt(II) and nickel(II) is shown in Scheme 3.

Electrochemistry studies were carried out on complexes **2** and **3**. For **3**, cyclic voltammetry in CH_2Cl_2 solution exhibits two monoelectronic reversible reduction waves (Figure 6, **B** and **C**) with half wave potentials at $E_{1/2}$ = −0.63 V/SCE and $E_{1/2}$ = −0.99 V/SCE which were determined by Rotating Disc Electrode and Cyclic Voltammetry (Table 3). They are followed by a last irreversible reduction at a peak potential value Ep = −1.53 V/SCE (**D** in Figure 6). The same reduction sets of peaks are observed with complex **2**. According to these observations, the two consecutive reduction waves **B** and **C** can be attributed to consecutive reduction of the coordinated ligands **HL3** in the complex leading to the formation of successive stable anion radical and dianion species in nonaqueous solvent (Scheme 4).

Upon oxidation, the cyclic voltammetry of complex **3** shows a supplementary monoelectronic reversible oxidation wave with a half wave potential $E_{1/2}$ = 0.29/SCE (**A** in Figure 6). The linear dependence of the peak current Ip versus the square root of the scan rate potential $\sqrt{V}$ between 0.05 and 0.3 V/s demonstrates a diffusion-controlled process. Moreover, the peak separation $\Delta Ep = Ep_{ox} - E_{pred}$ is equal to 0.11 at 0.05 V/s which is typical of a slow heterogeneous electron transfer on the GC electrode. The voltammogram under stationary conditions recorded during the forward−backward coulometry on the peak **A** shows that the oxidized and reduced form are stable in solution under an inert atmosphere in the time scale of

dx.doi.org/10.1021/ic202493z | Inorg. Chem. 2012, 51, 2588−2596

Scheme 3. Catalytic Oxidation of H_2L2 into HL3 in Presence of Nickel(II) or Cobalt(II) Salts

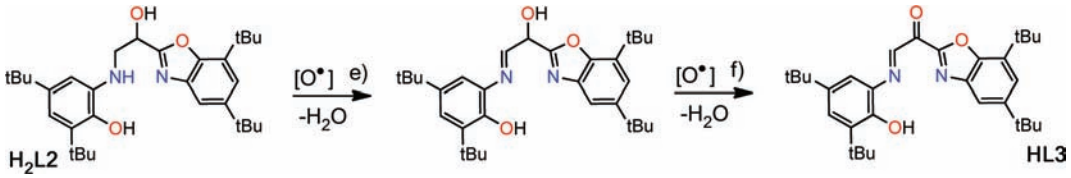

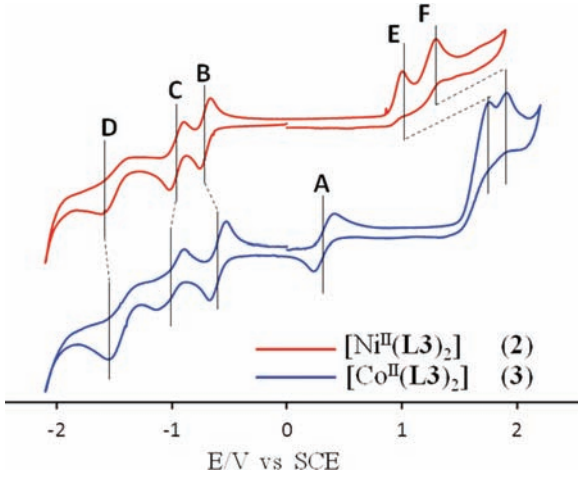

Figure 6. Cyclic voltammetry of **2** and **3** at GC electrode (3 mm diameter) in CH_2Cl_2 at 0.05 V/s.

Table 3. Electrochemical Data for 2 and 3[a]

	anodic peak potential ($E_{1/2}$)			cathodic peak potential ($E_{1/2}$)	
2	1.00[b]	1.30[b]		−0.74[c] (−0.71)	−1.02[c] (−0.97)
3	1.71[b]	1.86[b]	0.35[c] (0.29)	−0.67[c] (−0.63)	−1.05[c] (−0.99)

[a]Peak potential (V) and half wave potential $E_{1/2}$ recorded in CH_2Cl_2 at 293 K with a glassy carbon electrode, 0.1 M n-Bu_4NPF_6 as supporting electrolyte; all potentials are versus SCE, scan rate 0.05 V s^{-1}. [b]Irreversible system. [c]Reversible system.

Scheme 4. Redox Process Proposed for 2 (M = Ni^{II}) and 3 (M = Co^{II})

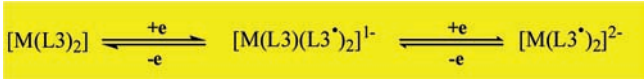

the electrolysis. By comparison, no oxidation peak exists in this potential region for the complex **2**. These results are characteristic of the redox process cobalt(III)/cobalt(II) in the complex **3**, which is interesting for future catalytic system studies.

Finally, two large and irreversible waves are recorded at larger positive potential (**E** and **F** in Figure 6) at 1.71 V/ECS and 1.86 V/ECS.

In this last similar potential domain, we observe two new successive monoelectronic and irreversible oxidation waves at 1.00 V/SCE and 1.30 V/SCE for complex **2**. The oxidation waves are associated with new reduction peaks of weak intensity at 0.28 V/ECS and 0.50 V/ECS respectively. This behavior is characteristic of a complicated oxidation mechanism.

$[Mn^{II}_4(HL4)_4Cl_4]$ (**4**) was also obtained from H_2L2 as colorless needle-like crystals when H_2L2 was reacted with $MnCl_2{\cdot}4H_2O$ in a 1:1 ratio in acetonitrile. It crystallizes in monoclinic space group $C2/c$. The crystal structure consists of cubane-like discrete molecules (Figure 7).

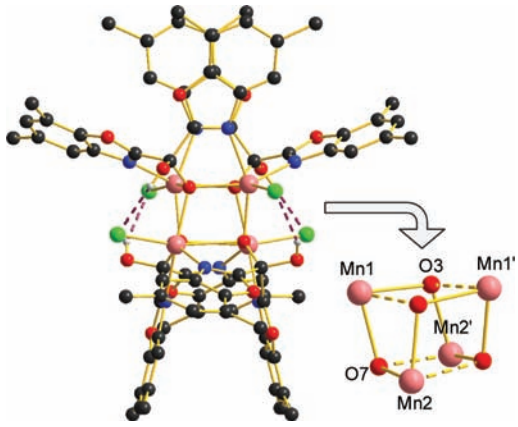

Figure 7. Molecular structure of **4** with cubane "4 + 2" cluster core. Methyl groups and hydrogen atoms are omitted for clarity.

The reaction of H_2L2 with manganese(II) ions causes a more significant modification in the structure of the initial ligand compared with cobalt(II) and nickel(II) based compounds. Indeed, the X-ray crystal structure of **4** shows that, in the manganese(II) complex, a new ligand H_2L4 containing a second benzoxazole ring and an additional OH group is obtained (Figure 8). The further oxidation of **HL3** into H_2L4

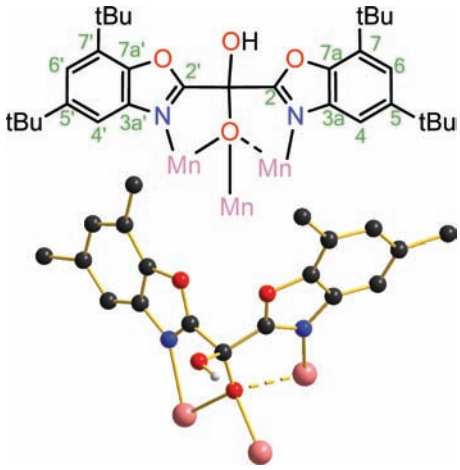

Figure 8. Coordination mode of H_2L4 in **4**.

could be ascribed to a stronger catalytic activity of manganese(II) ions. After the formation of **HL3** (Scheme 3) the cyclization of the second benzoxazole ring takes place (Scheme 5g) and the intermediate ketone in the equilibrium with water gives the bis-hydroxyl compound (Scheme 5h), as may be observed for pyridine-ketones.[60−62] A similar formation of two benzoxazole rings was reported when the condensation product

dx.doi.org/10.1021/ic202493z | Inorg. Chem. 2012, 51, 2588−2596

Scheme 5. Catalytic Oxidation of HL3 into H_2L4 in Presence of Manganese(II) Salts

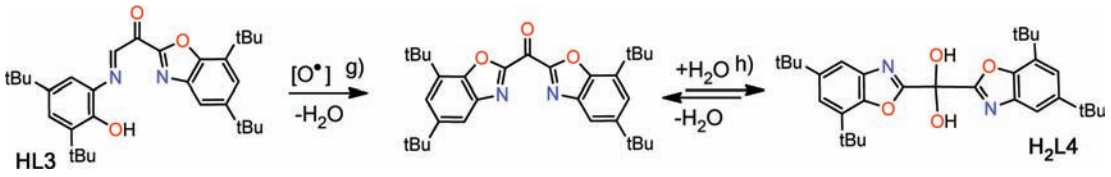

of DTBBQ with 2,2-dimethylpropylenediamine was reacted with $PdCl_2$ in methanol.[20]

The coordination mode of **H_2L4** in **4** is presented in Figure 8. The core of the cluster is formed by four manganese(II) ions arranged in a cubane-like "4 + 2" fashion.[63] Central atoms are bridged together by alkoxo groups of four monodeprotonated **H_2L4** ligands. The geometry of manganese(II) ions is square-based pyramidal with two bridging alkoxo groups and two nitrogen atoms of **H_2L4** in the basal plane and a chlorine ion in the apical position with bond lengths of 2.143−2.170 Å, 2.179−2.284 Å, and 2.390−2.395 Å for Mn−O, Mn−N, and Mn−Cl, respectively.

The magnetic properties studies of **4** are shown in Figure 9 under the form of χ_M and $\chi_M T$ versus T plot. At room

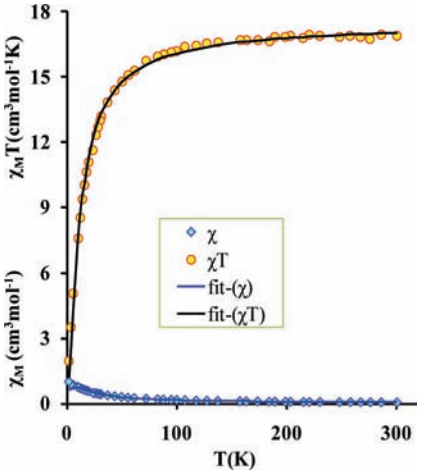

Figure 9. $\chi_M T$ and χ_M versus T plot for **4**. The solid lines indicate the best fit of the data with the theoretical model with the parameters indicated in the text.

temperature, the value of the $\chi_M T$ product (H = 0.1 T) is 16.88 cm^3 K mol^{-1} (Figure 9) which is lower than the value of 17.50 cm^3 K mol^{-1} expected for four noninteracting manganese(II) ions (S = 5/2, g = 2). Upon cooling $\chi_M T$ decreases continuously down to 1.97 cm^3 K mol^{-1} at 2 K, indicating dominant antiferromagnetic Mn^{II}−Mn^{II} interactions within the tetranuclear complex.

The general spin-Hamiltonian we used to describe the isotropic exchange interactions within the tetranuclear complex is given by the following expression:

$$H = -2(J_{12}S_1S_2 + J_{23}S_2S_3 + J_{34}S_3S_4 + J_{14}S_1S_4 + J_{13}S_1S_3 + J_{24}S_2S_4)$$

In this case S_1=S_2=S_3=S_4 = 5/2. As described above, the molecular structure of **4** consists of a "4 + 2" cubane-like arrangement of manganese(II) ions[63] (Figure 7). While the magnetic exchange interactions between each pair S_1S_2, S_2S_3, S_3S_4, S_1S_4 may be considered nearly equivalent ($J_a = J_{12} = J_{23} = J_{34} = J_{14}$), we neglected the magnetic interactions between S_1S_3 and S_2S_4 ($J_{13} = J_{24} = 0$) to simplify the following calculations. Thus, the final expression of Hamiltonian used to describe the exchange interactions in **4** is

$$H = -2J_a(S_1S_2 + S_2S_3 + S_3S_4 + S_1S_4)$$

A similar approach has been widely used for magnetic characterization of homo- and heterometallic spin clusters like $[Cr_4(\mu_3\text{-}O)_2]$,[64] $[V_4(\mu_3\text{-}O)_2]$,[65] $[Fe_4(\mu_3\text{-}O)_2]$,[66−71] $[Fe_2Mn_2(\mu_3\text{-}O)_2]$,[72] $[Cr_2Mn_2(\mu_3\text{-}O)_2]$,[72] $[Cr_2Fe_2(\mu_3\text{-}O)_2]$[66] including homovalence $[Mn^{III}{}_4(\mu_3\text{-}O)_2]$ and mixed-valence $[Mn^{III}{}_2Mn^{II}{}_2(\mu_3\text{-}O)_2]$[71−81] clusters.

A satisfactory fit of the experimental data for compound **4** (Figure 9) was obtained with parameters $J_a(Mn^{II}\text{-}Mn^{II})$ = −0.50(1) cm^{-1}; g = 2.00(7) and zJ = 0.0 (fix) cm^{-1} where zJ holds for intermolecular interactions. The value for magnetic interactions is consistent with previously reported alkoxo bridged Mn^{II}−Mn^{II}.

CONCLUSION

In summary, we report the synthesis and characterization of two benzoxazoles derivative ligands resulting from the condensation of 3,5-di-*tert*-butyl-*o*-benzoquinone (DTBBQ) with ethanolamine or 1,3-diamino-2-hydroxypropane in methanol. With ethanolamine we obtained the expected methylenhydroxylbenzoxazole (**HL1**). In contrast with 1,3-diamino-2-hydroxypropane the condensation of DTBBQ occurs with the two amino groups but the successive process results in a benzoxazole ring only on one side to give **H_2L2** instead of the symmetric *bis*-benzoxazole derivative. The structure of **HL1** and **H_2L2** was confirmed by NMR-spectroscopy and X-ray diffraction. Their ability to coordinate was checked for both ligands. The reaction of **HL1** with $CuCl_2$ gives rise to a mononuclear **$[Cu^{II}(HL1)_2Cl_2]$** (**1**) complex, while the use of a mixture of copper(II) and lanthanide (III) salts results in heterometallic dodecanuclear complexes $[Ln_4Cu_8]$, as we have previously reported.[42] The structure of the **HL1** does not change upon the reaction with Cu^{II} or Cu^{II}/Ln^{III} ions as shown by X-ray crystal structure. The reaction of **H_2L2** with nickel(II), cobalt(II), and manganese(II) salts were also studied. The X-ray crystal structure show that during reaction with transition metal ions the initial **H_2L2** undergoes versatile chemical transformation to give **HL3** in mononuclear complexes **$[M^{II}(L3)_2]$** (M = Ni^{II} (**2**); M = Co^{II} (**3**)) and **H_2L4** in the tetranuclear complex **$[Mn^{II}{}_4(HL4)_4Cl_4]$** (**4**). These results demonstrate that benzoxazole based ligands as **H_2L2** possess interesting redox activity and can be selectively oxidized using different transition metal ions. We believe that these results give some new insights in the domain of benzoxazole based compounds, which is complicated, quite unpredictable, and still not very well studied but give promising perspectives.

dx.doi.org/10.1021/ic202493z | Inorg. Chem. 2012, 51, 2588−2596

■ ASSOCIATED CONTENT

Supporting Information

Crystallographic refinement details for **HL1** and **1**−**4**. This material is available free of charge via the Internet at http://pubs.acs.org.

■ AUTHOR INFORMATION

Corresponding Author

*E-mail: luneau@univ-lyon1.fr.

■ ACKNOWLEDGMENTS

O.I. thanks the "French Ministry of Education" for Ph.D. grant. G.N. thanks the Marie Curie Actions (FP7-People-IIF) for financial support. D.L. thanks the *Laboratoire des Champ Magnétique Intenses* in Grenoble, where this work was initiated, for hosting a part of his group while refurnishing his chemical rooms in Lyon. X-ray diffraction studies on single crystals were done at the Centre de Diffraction Henri Longchambon at Université Claude Bernard.

■ REFERENCES

(1) Harry, B. G. *Coord. Chem. Rev.* **1966**, *1*, 156−163.
(2) Jorgensen, C. K. *Coord. Chem. Rev.* **1966**, *1*, 164−178.
(3) Pierpont, C. G.; Buchanan, R. M. *Coord. Chem. Rev.* **1981**, *38*, 45−87.
(4) Pierpont, C. G. *Coord. Chem. Rev.* **2001**, *216*−*217*, 99−125.
(5) Pierpont, C. G. *Coord. Chem. Rev.* **2001**, *219*−*221*, 415−433.
(6) Chaudhuri, P.; Wieghardt, K. Phenoxyl radical complexes. In *Progress in Inorganic Chemistry*; Wiley: New York, **2001**; Vol. *50*, pp 151−216.
(7) Dei, A.; Gatteschi, D.; Sangregorio, C.; Sorace, L. *Acc. Chem. Res.* **2004**, *37*, 827−835.
(8) Hendrickson, D. N.; Pierpont, C. G.; Gutlich, P.; Goodwin, H. A. Valence Tautomeric Transition Metal Complexes. In *Spin Crossover in Transition Metal Compounds II*; Springer: Berlin, 2004; Vol. *234*, pp 786−786.
(9) Hendrickson, D. N.; Pierpont, C. G. In *Spin Crossover in Transition Metal Compounds II*; Springer: Berlin, 2004, Vol. *234*, pp 6395
(10) Sato, O.; Cui, A.; Matsuda, R.; Tao, J.; Hayami, S. *Acc. Chem. Res.* **2007**, *40*, 361−369.
(11) Chirik, P. J. *Inorg. Chem.* **2011**, *50*, 9737−9740.
(12) Kaim, W. *Inorg. Chem.* **2011**, *50*, 9752−9765.
(13) Verma, P.; Weir, J.; Mirica, L.; Stack, T. D. P. *Inorg. Chem.* **2011**, *50*, 9816−9825.
(14) Pierpont, C. G. *Inorg. Chem.* **2011**, *50*, 9766−9772.
(15) Scarborough, C. C.; Wieghardt, K. *Inorg. Chem.* **2011**, *50*, 9773−9793.
(16) Heinze-Bruckner, G.; Walleck, S.; Strautmann, J. B. H.; Stammler, A.; Bogge, H.; Glaser, T. *Inorg. Chim. Acta* **2011**, *374*, 385−391.
(17) Strautmann, J. B. H.; von Richthofen, C. G. F.; Heinze-Bruckner, G.; DeBeer, S.; Bothe, E.; Bill, E.; Weyhermuller, T.; Stammler, A.; Bogge, H.; Glaser, T. *Inorg. Chem.* **2011**, *50*, 155−171.
(18) Glaser, T.; Pawelke, R. H.; Heidemeier, M. *Z. Anorg. Allg. Chem.* **2003**, *629*, 2274−2281.
(19) Strautmann, J. B. H.; von Richthofen, C. G. F.; George, S. D.; Bothe, E.; Bill, E.; Glaser, T. *Chem. Commun.* **2009**, 2637−2639.
(20) Min, K. S.; Weyhermuller, T.; Bothe, E.; Wieghardt, K. *Inorg. Chem.* **2004**, *43*, 2922−2931.
(21) Benisvy, L.; Wanke, R.; da Silva, M.; Pombeiro, A. J. L. *Eur. J. Inorg. Chem.* **2011**, 2791−2796.
(22) Mollo, L.; Levresse, V.; Ottaviani, M. F.; ElloukAchard, S.; Jaurand, M. C.; Fubini, B. *Environ. Health Perspect.* **1997**, *105*, 1031−1036.
(23) Su, X.-C.; Otting, G. *J. Biomol. NMR* **2010**, *46*, 101−112.
(24) Eaton, D. R.; Watkins, J. M.; Buist, R. J. *J. Am. Chem. Soc.* **1985**, *107*, 5604−5609.
(25) Klare, J. P.; Ortiz de Orue Lucana, D., *Antioxid. Redox Signaling* **2011**.
(26) Beaumont, S. p.; Ilardi, E. A.; Monroe, L. R.; Zakarian, A. *J. Am. Chem. Soc.* **2011**, *132*, 1482−1483.
(27) Dzik, W. I.; Zhang, X. P.; de Bruin, B. *Inorg. Chem.* **2011**, *50*, 9896−9903.
(28) Sakaguchi, S.; Nishiwaki, Y.; Kitamura, T.; Ishii, Y. *Angew. Chem., Int. Ed.* **2001**, *40*, 222−224.
(29) Tsujimoto, S.; Iwahama, T.; Sakaguchi, S.; Ishii, Y. *Chem. Commun.* **2001**, 2352−2353.
(30) Ishii, Y.; Sakaguchi, S. *Catal. Today* **2006**, *117*, 105−113.
(31) Speier, G.; Csihony, J.; Whalen, A. M.; Pierpont, C. G. *Inorg. Chem.* **1996**, *35*, 3519−3524.
(32) Speier, G.; Tyeklár, Z.; Tóth, P.; Speier, E.; Tisza, S.; Rockenbauer, A.; Whalen, A. M.; Alkire, N.; Pierpont, C. G. *Inorg. Chem.* **2001**, *40*, 5653−5659.
(33) Berreau, L. M.; Mahapatra, S.; Halfen, J. A.; Houser, R. P.; Young, J. V. G.; Tolman, W. B. *Angew. Chem., Int. Ed.* **1999**, *38*, 207−210.
(34) Ye, S.; Sarkar, B.; Niemeyer, M.; Kaim, W. *Eur. J. Inorg. Chem.* **2005**, *2005*, 4735−4738.
(35) Dei, A.; Gatteschi, D.; Pardi, L.; Barra, A. L.; Brunel, L. C. *Chem. Phys. Lett.* **1990**, *175*, 589−592.
(36) Dei, A.; Gatteschi, D.; Pardi, L. *Inorg. Chem.* **1993**, *32*, 1389−1395.
(37) Carbonera, C.; Dei, A.; Létard, J. F.; Sangregorio, C.; Sorace, L. *Angew. Chem., Int. Ed.* **2004**, *43*, 3136−3138.
(38) Corey, E. J.; Achiwa, K. *J. Am. Chem. Soc.* **1969**, *91*, 1429−1432.
(39) Vinsova, J.; Horak, V.; Buchta, V.; Kaustova, J. *Molecules* **2005**, *10*, 783−793.
(40) Cherkasov, V.; Druzhkov, N.; Kocherova, T.; Fukin, G.; Shavyrin, A. *Tetrahedron* **2011**, *67*, 80−84.
(41) Vinsova, J.; Horak, V. *Chemicke Listy* **2003**, *97*, 1157−1167.
(42) Iasco, O.; Novitchi, G.; Jeanneau, E.; Wernsdorfer, W.; Luneau, D. *Inorg. Chem.* **2011**, *50*, 7373−7375.
(43) Muto, M.; Hatae, N.; Tamekuni, Y.; Yamada, Y.; Koikawa, M.; Tokii, T. *Eur. J. Inorg. Chem.* **2007**, 3701−3709.
(44) Pascal, P. *Ann. Chim. Phys.* **1910**, *19*, 5.
(45) Kahn, O. *Molecular Magnetism*; VCH Publishers, Inc: New York, 1993.
(46) Yerly, F. *VISUALISEUR-OPTIMISEUR*; EPFL: Lausanne, Switzerland, 2003.
(47) *MATLAB*; The MathWorks Inc.: Natick, MA, 2000.
(48) Clark, R. C.; Reid, J. S. *Acta Crystallogr., Sect. A* **1995**, *51*, 887−897.
(49) Cosier, J.; Glazer, A. M. *J. Appl. Crystallogr.* **1986**, *19*, 105−107.
(50) Altomare, A.; Burla, M. C.; Camalli, M.; Cascarano, G. L.; Giacovazzo, C.; Guagliardi, A.; Moliterni, A. G. G.; Polidori, G.; Spagna, R. *J. Appl. Crystallogr.* **1999**, *32*, 115−119.
(51) Betteridge, P. W.; Carruthers, J. R.; Cooper, R. I.; Prout, K.; Watkin, D. J. *J. Appl. Crystallogr.* **2003**, *36*, 1487.
(52) *DIAMOND*, 2.1d; Crystal Impact GbR, Brandeburg and Putz: Bonn, Germany, 2000.
(53) Horak, V.; Mermersky, Y. *e-EROS Encyclopedia of Reagents for Organic Synthesis*.; CAPLUS-database, 2001.
(54) Bersuker, I.; Bersuker, I. B. *The Jahn-Teller Effect*; Cambridge University Press: New York, 2006.
(55) Stephens, F. F.; Bower, J. D. *J. Chem. Soc.* **1950**, 1722−1726.
(56) Stephens, F. F.; Bower, J. D. *J. Chem. Soc.* **1949**, 2971−2972.
(57) Uzarevic, K.; Rubcic, M.; Stilinovic, V.; Kaitner, B.; Cindric, M. *J. Mol. Struct.* **2010**, *984*, 232−239.
(58) Zhang, X. H.; Zummack, W.; Schroder, D.; Weinhold, F. A.; Schwarz, H. *Chem.—Eur. J.* **2009**, *15*, 11815−11819.
(59) Ziolek, M.; Kubicki, J.; Maciejewski, A.; Naskrecki, R.; Grabowska, A. *J. Chem. Phys.* **2006**, 124.
(60) Stoumpos, C. C.; Stamatatos, T. C.; Psycharis, V.; Raptopoulou, C. P.; Christou, G.; Perlepes, S. P. *Polyhedron* **2008**, *27*, 3703−3709.

(61) Stoumpos, C. C.; Gass, I. A.; Milios, C. J.; Kefalloniti, E.; Raptopoulou, C. P.; Terzis, A.; Lalloti, N.; Brechin, E. K.; Perlepes, S. P. *Inorg. Chem. Commun.* **2008**, *11*, 196−202.
(62) Dendrinou-Samara, C.; Alexiou, M.; Zaleski, C. M.; Kampf, J. W.; Kirk, M. L.; Kessissoglou, D. P.; Pecoraro, V. L. *Angew. Chem., Int. Ed.* **2003**, *42*, 3763−3766.
(63) Ruiz, E.; Rodriguez-Fortea, A.; Alemany, P.; Alvarez, S. *Polyhedron* **2001**, *20*, 1323−1327.
(64) Bino, A.; Chayat, R.; Pedersen, E.; Schneider, A. *Inorg. Chem.* **1991**, *30*, 856−858.
(65) Castro, S. L.; Sun, Z. M.; Grant, C. M.; Bollinger, J. C.; Hendrickson, D. N.; Christou, G. *J. Am. Chem. Soc.* **1998**, *120*, 2365−2375.
(66) Chaudhuri, P.; Winter, M.; Fleischhauer, P.; Haase, W.; Florke, U.; Haupt, H.-J. *Inorg. Chim. Acta* **1993**, *212*, 241−249.
(67) McCusker, J. K.; Vincent, J. B.; Schmitt, E. A.; Mino, M. L.; Shin, K.; Coggin, D. K.; Hagen, P. M.; Huffman, J. C.; Christou, G.; Hendrickson, D. N. *J. Am. Chem. Soc.* **1991**, *113*, 3012−3021.
(68) Boudalis, A. K.; Lalioti, N.; Spyroulias, G. A.; Raptopoulou, C. P.; Terzis, A.; Bousseksou, A.; Tangoulis, V.; Tuchagues, J.-P.; Perles, S. P. *Inorg. Chem.* **2002**, *41*, 6474−6487.
(69) Boudalis, A. K.; Tangoulis, V.; Raptopoulou, C. P.; Terzis, A.; Tuchagues, J.-P.; Perles, S. P. *Inorg. Chim. Acta* **2004**, *357*, 1345−1354.
(70) Glaser, T.; Lugger, T. *Inorg. Chim. Acta* **2002**, *337*, 103−112.
(71) Lan, Y.; Novitchi, G.; Clerac, R.; Tang, J. K.; Madhu, N. T.; Hewitt, I. J.; Anson, C. E.; Brooker, S.; Powell, A. K. *Dalton Trans.* **2009**, 1721−1727.
(72) Chaudhuri, P.; Eva, R.; Birkelbach, F.; Krebs, C.; Bill, E.; Weyhermuller, T.; Florke, U. *Eur. J. Inorg. Chem.* **2003**, 541−555.
(73) Albela, B.; Fallah, M. S. E.; Ribas, J.; Folting, K.; Christou, G.; Hendrickson, D. N. *Inorg. Chem.* **2001**, *40*, 1037−1044.
(74) Wittick, L. M.; Murray, K. S.; Moubaraki, B.; Batten, S. R.; Spiccia, L.; Berry, K. J. *Dalton Trans.* **2004**, 1003−1011.
(75) Wemple, M. W.; Tsai, H.-L.; Wang, S.; Claude, J. P.; Streib, W. E.; Huffman, J. C.; Hendrickson, D. N.; Christou, G. *Inorg. Chem.* **1996**, *35*, 6437−6449.
(76) Wittick, L. M.; Jones, L. F.; Jensen, P.; Moubaraki, B.; Spiccia, L.; Berry, K. J.; Murray, K. S. *Dalton Trans.* **2006**, 1534−1543.
(77) Bagai, R.; Abboud, K. A.; Christou, G. *Dalton Trans.* **2006**, 3306−3312.
(78) Miyasaka, H.; Nakata, K.; Lecren, L.; Coulon, C.; Nakazawa, Y.; Fujisaki, T.; Sugiura, K.; Yamashita, M.; Clerac, R. *J. Am. Chem. Soc.* **2006**, *128*, 3770−3783.
(79) Vincent, J. B.; Christmas, C.; Chang, H. R.; Li, Q. Y.; Boyd, P. D. W.; Huffman, J. C.; Hendrickson, D. N.; Christou, G. *J. Am. Chem. Soc.* **1989**, *111*, 2086−2097.
(80) Yang, C.-I.; Lee, G.-H.; Wur, C.-S.; Lin, J. G.; Tsai, H. L. *Polyhedron* **2005**, *24*, 2215−2221.
(81) Canada-Vilalta, C.; Huffman, J. C.; Christou, G. *Polyhedron* **2001**, *20*, 1785−1793.